Applied problems of nonlinear oscillation and wave theory

Official English translation

ANALYSIS OF SYNCHRONOUS MODES OF COUPLED OSCILLATORS IN POWER GRIDS

P. A. Arinushkin, V. S. Anishchenko

Saratov State University
83, Astrakhanskaya, 410012 Saratov, Russia
E-mail: arinushkin.pavel@gmail.com, wadim@info.sgu.ru
Received 12.03.2018

Aim. The aim of the study is to formulate an effective model of the power grid, to determine the stable modes of its operation, to identify differences in the considered modes and to test the stability of the system to changes in control parameters, initial conditions and to various types of external influence. **Method**. The effective model of the energy network, which consists of three coupled oscillators, is considered for different methods of setting the initial conditions and variation of the control parameters. Numerical simulation of power systems allows to reveal the steady states of the oscillators, at which the stable operation of power systems is observed. This approach makes it possible to optimize power systems, to determine the mechanisms for improving the stability of the system and to identify the parts of power systems, that are more prone to negative factors. In the framework of our study, the operating modes of the power grid are compared under the influence of external noise of different intensities and rectangular pulses, which simulate power surges in the power grid. **Results**. The effective model of the power system consisting of three coupled generators has been proposed and numerically explored. It is shown that when the output power of the generator is changed, a regime which is resistant to variations of the initial conditions can be obtained. It is found that the functioning of such a system is less sensitive to various external factors. In particular, the mode with synchronization of phase velocities of all the oscillators is more resistant to power consumption changes, noise effects and transmission line breaks in comparison with the mode of synchronization with different phase velocities. **Discussion**. The study of the power grid of three coupled generators has demonstrated the behavior of the key modes of operation of the power grids and has shown the possibility for optimizing the network by adjusting the generator output power parameter. In this paper, we have considered the synchronization of power grid for only one model of the network. As a further study of networks, it is necessary to conduct a comparative analysis of synchronization modes of several power grid models.

Key words: power grids, synchronous machines, phase oscillators, synchronization of coupled generators, stability of dynamic modes.

DOI: 10.18500/0869-6632-2018-26-3-62-77

Reference: Arinushkin P.A., Anishchenko V.S. Analysis of synchronous modes of coupled oscillators in power grids. *Izvestiya VUZ, Applied Nonlinear Dynamics,* 2018, vol. 26, no. 3, pp. 62–77. DOI: 10.18500/0869-6632-2018-26-3-62-77

Introduction and problem statement

Nowadays it is crucial to provide technical solutions to overcome the power grid stability challenges. It implies the advanced knowledge in electrical engineering and design and thorough consideration of dynamic processes between power plants and consumers. The ever-expanding circle of consumers entails an increased number of power sources, further complicating the task of fostering the sustainability of the power grid. Moreover, the emergence of renewable energy sources makes their integration with high-powered electrical grids, that include turbogenerators, a priority [1]. The power grid is monitored through data collection and controlled by the operator. Such an approach is less effective than an ongoing monitoring of power grids and computer automation of the processes. Quick decision-making process and grid resilience in the emergency mode are the key issues for power grid stability. Another solution to the problem might be computer modeling and the application of optimization modeling techniques, which involve a set of stress-tests to analyze the vulnerability and stability of the grid.

With the advent of synchronous machines as production sources of power in power grids, concerns have emerged regarding the stability and sustainability of electrical power generators. Synchronous machines are the basic elements in the construction of the power plants. Due to the restrictions of output capacity of these facilities and the increased consumption, there is a need for additional electricity supply. Thus, a power grid is a complex system consisting of multiple generators and consumers. It is also worth noting that renewable energy sources are responsible for the heterogeneous topology of the power grids [2], thus making it difficult to determine the steady-state stability of synchronous machines. Another challenge is to ensure minimum losses and rational distribution of power provided by different sources between the consumers [3–5]. Thus, the main objectives of the study of power grids are optimized energy distribution between the consumers and their grid resilience in the emergency mode and against other factors that may impair electrical power generators.

Consider the simplest model of the electric power system [6], consisting of an equivalent generator (synchronous machine), an output node of the generator (transformer), and a transmission line (Fig. 1, *a*).

Let's introduce the following constraint: the transmission line is connected to the massive power system through an infinite bus. This implies that the output voltage module and the output frequency are regarded as invariable. Let's simplify the layout by eliminating the effect of capacitance and active impedance of the transmission line (Fig. 1, *b*). Consider the synchronous EMF of the generator E_q connected to the source of voltage U through the equivalent

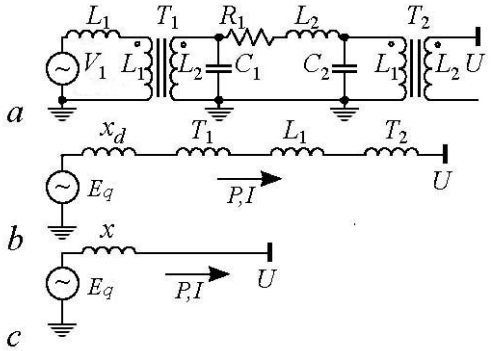

Fig. 1. Network layout for one synchronous machine: (*a*) schematic diagram of the one-machine system; (*b*) simplification of the circuit while eliminating the effect of capacitance and active resistance of the transmission line; (*c*) schematic diagram with a generalization of all inductances into a single inductance

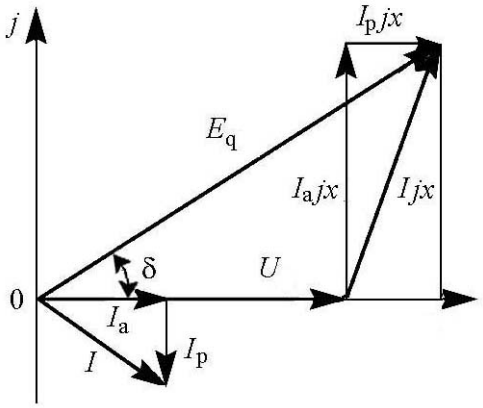

Fig. 2. Vector diagram of the synchronous machine parameters

inductance x (Fig. 1, *c*). Equivalent inductance is the sum of all inductances of all the elements involved:

$$x = x_d + x_{\mathrm{T1}} + x_{\mathrm{L}} + x_{\mathrm{T2}}, \qquad (1)$$

where x_d is the transient inductive resistance of the generator; x_{T1} and x_{T2} are equivalent inductances of transformers T_1 and T_2, respectively; x_{L} is the equivalent inductance of the transmission line.

Consider the relationship between the capacity P and the values E_q and U, shown in the vector diagram of voltages and currents (Fig. 2). The diagram shows that the values E_q and U are determined by the angle δ between them. Next we expand the diagram with the active I_a and reactive I_p components of current I and active $I_a jx$ and reactive $I_p jx$ components of the voltage drop Ijx at the equivalent resistance x. The resulting equation is:

$$I_{\mathrm{a}} x = E_q \sin\delta. \qquad (2)$$

Multiplying both sides of the equation (2) by $3U/x$ and taking into account that the three-phase power is equal to $P = 3UI_{\mathrm{a}}$, for single-phase power P_{e} we obtain:

$$P_{\mathrm{e}} = \frac{E_q U}{x} \sin\delta. \qquad (3)$$

With constant values $E_q = \mathrm{const}$ and $U = \mathrm{const}$ equation (2) is a sinusoidal function of the active capacity of the generator, which depends on the angle. Now rewrite the swing equation (see Annex) by adding an expression for P_{e}:

$$\frac{2H}{\omega_R}\ddot{\delta} + \frac{D}{\omega_R}\dot{\delta} = P_{\mathrm{m}} - \frac{E_q U}{x_d} \sin\delta. \qquad (4)$$

The equation (4) represents the electromechanical description of power imbalance in the swing equation (see Sec. 4)) and we will use precisely this representation of the model in the study of the single and collective dynamics of synchronous machines.

1. Equations of an effective network model for the chain of three coupled oscillators

Consider the structure and parameters of the network, which consists of nine elements (Fig. 3, *a*). The total number of elements is defined as $N{=}2n_g{+}n_l$, where n_g denotes elements that belong to generators (since generators are always represented through the output nodes of the transformers, the total number of generators is doubled); n_l stands for the total number of the network load elements.

To simplify the differential equations, we use the effective network method presented in [7]. The method is based on eliminating from consideration the network load, on the condition that the electric power load consumption does not change over time $P_i + jQ_i$= const. By applying this method to a physical network, we get an efficient network, which topology contains no loads. Thus, we are able to consider only the interaction of coupled generators (Fig. 3, *b*). Transformation of such a network is carried out using Kron reduction for the initial conductance matrix of the physical network [8].

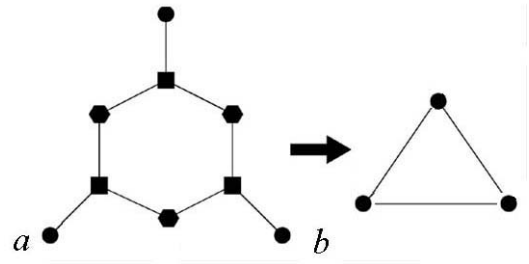

Fig. 3. Scheme of transformation of a physical network to an effective network model: topology of the physical network (*a*); topology of the effective network model (*b*); the generators are denoted by a circle, the output nodes (transformers) – by a square and the constant power grid loads – by a hexagon

The algorithm for the conductance matrix transformation is described in the MATPOWER software package [9]. The transmission lines between the physical network nodes are seen as a set of values for the overall conductivities. Since there is a heterogeneous network with nodes of different connectivity, it should be taken into account when calculating the conductance matrix. Then using the software package, the parameters of active generator power P_{gi}, reactive generator power Q_{gi}, the output node voltage of the transformer V_i and its phase φ_i are obtained. As a result, we get the complete physical network configuration, which is necessary to form a simplified topology, and the model parameters of the effective network. Therefore, the effective network model takes the form:

$$\frac{2H_i}{\omega_R}\ddot{\delta}_i + \frac{D_i}{\omega_R}\dot{\delta}_i = A_i^{\mathrm{EN}} - \sum_{j=1,j\neq i}^{n_g} K_{ij}^{\mathrm{EN}} \sin(\delta_i - \delta_j - \gamma_{ij}^{\mathrm{EN}}), \quad i = 1, \cdots, n_g \quad (5)$$

$$A_i^{\mathrm{EN}} = P_{g,i} - |E_i|^2 G_{ii}^{\mathrm{EN}}, \quad K_{ij}^{\mathrm{EN}} = |E_i E_j Y_{ij}^{\mathrm{EN}}|, \quad \gamma_{ij}^{\mathrm{EN}} = \alpha_{ij}^{\mathrm{EN}} - \frac{\pi}{2}, \quad (6)$$

where ω_R is the reference angular frequency of the system; H_i and D_i are the constants of inertia and damping of the oscillators, respectively; A_i stands for the parameters of the pure generation capacity; the parameters K_{ij} represent the dynamic connection of the coupled oscillators i and j or maximums of reciprocal capacity of the generators and receiving systems; γ_{ij} denotes phase shifts between the corresponding oscillators. All the abovementioned system parameters are given in the dimensionless form. The basic capacity $P_R = 100$ MVA is used as the normalizing value.

The network frequency $\omega_R = 50$ Hz or 314.1593 rad/s was taken as a system reference frequency. The values of the inertia constant and the transient inductive resistance of the generator can be approximated by the formulas $H_i = 0.04P_i$ and $x_d = 92.8P_i^{-1.3}$, respectively. Next we calculate the combined dissipation parameter as follows $D_i = (D_{\mathrm{m}i} + D_{\mathrm{e}i} + 1/R_i)(\omega_R/P_R)$, where the mechanical friction of the rotor shaft ($D_{\mathrm{m}i} = 0$) and the electric parasitic effect of the generator stator windings ($D_{\mathrm{e}i} = 0$) are negligible. It now remains to examine the parameter that defines the reference frequency of the generator as $R_i = 0.02\omega_R/P_R = 0.0628$. Substituting this value into the generalized dissipation parameter yields $D_i = 50$. Consider an example where damping parameter is completely absent, that is, $D_i = 0$. Consequently the reference frequency of

the generator is not controlled by the control system and its value may differ considerably from the network frequency. At the same time, however, the rotor of the synchronous machine is selfexcited, thus constantly changing the rotation speed and, more often than not, disrupting the steady-state operation of the generator [10].

Further we define the parameters A_i, K_{ij} and γ_{ij} in the right-hand side of the equations. Thus, it is necessary to transform the conductance matrix of a physical network Y_0 into the matrix of an effective network Y^{EN}.

$$Y_0 = \begin{pmatrix} Y^{gg} & Y^{gl} \\ Y^{lg} & Y^{ll} \end{pmatrix} \tag{7}$$

Here Y^{gg}, Y^{gl}, Y^{lg}, Y^{ll} are the conductance sets of the network elements, grouped with regard to the intrinsic and mutual conductivities of the transmission line of generators and network loads. We supplement the given matrix with the component Y_d, that consists of the diagonal elements of the transient resistances of the generators' inductances $(jx_d, 1)^{-1} \cdots (jx_d, n_g)^{-1}$, where n_g is the total number of generators. Providing that the shunting conductivity $Y^{l,i}$ is equivalent to the load $Y^{l,i} = (P^{l,i} - jQ^{li})/|V_i|^2$, the components $\bar{Y}^{gg}$ and $\bar{Y}^{ll}$ are determined as $\bar{Y}^{gg} = Y^{gg} + Y^{li}$ и $\bar{Y}^{ll} = Y^{ll} + Y^{li}$, we obtain the final form of the matrix:

$$Y_0 = \begin{pmatrix} Y_d & -Y_d & 0 \\ -Y_d & \bar{Y}^{gg} + Y_d & Y^{gl} \\ 0 & Y^{lg} & \bar{Y}^{ll} \end{pmatrix}. \tag{8}$$

Finally, we define the desired elements of the effective matrix using Kron reduction in accordance with the formula $Y^{\mathrm{EN}} = Y'(1 + Y_d^{-1}Y')^{-1}$, where $Y' = \bar{Y}^{gg} - Y^{gl}(\bar{Y}^{ll})^{-1}Y^{lg}$. Using this matrix, we determine the parameters for three generator nodes under investigation via the effective network method:

$$A_1^{\mathrm{EN}} = P_{g1} - |E_1|^2 G_{11}^{\mathrm{EN}}, \quad A_2^{\mathrm{EN}} = P_{g2} - |E_2|^2 G_{22}^{\mathrm{EN}}, \quad A_3^{\mathrm{EN}} = P_{g3} - |E_3|^2 G_{33}^{\mathrm{EN}}, \tag{9}$$

$$K_{12}^{\mathrm{EN}} = |E_1 E_2 Y_{12}^{\mathrm{EN}}|, \quad K_{13}^{\mathrm{EN}} = |E_1 E_3 Y_{13}^{\mathrm{EN}}|, \quad K_{23}^{\mathrm{EN}} = |E_2 E_3 Y_{23}^{\mathrm{EN}}|, \tag{10}$$

$$\gamma_{12}^{\mathrm{EN}} = \alpha_{12}^{\mathrm{EN}} - \frac{\pi}{2}, \quad \gamma_{13}^{\mathrm{EN}} = \alpha_{13}^{\mathrm{EN}} - \frac{\pi}{2}, \quad \gamma_{23}^{\mathrm{EN}} = \alpha_{23}^{\mathrm{EN}} - \frac{\pi}{2}, \tag{11}$$

where P_{gi} is the active capacity *i* of the generator; G_{ii}^{EN} is the real part of the diagonal elements of the effective matrix Y^{EN}; E_i and E_j are synchronous EMF of the coupled generators; $\alpha_{ij}^{\mathrm{EN}}$ is the phase angle $|Y_{ij}^{\mathrm{EN}}|e^{j\alpha}$, that is responsible for the angular displacement of the synchronous machine.

As a result, we get the equations for the system under consideration

$$\begin{cases} \dfrac{2H_1}{\omega_R}\ddot{\delta}_1 + \dfrac{D_1}{\omega_R}\dot{\delta}_1 = A_1^{\mathrm{EN}} - K_{12}^{\mathrm{EN}}\sin(\delta_1-\delta_2-\gamma_{12}^{\mathrm{EN}}) - K_{13}^{\mathrm{EN}}\sin(\delta_1-\delta_3-\gamma_{13}^{\mathrm{EN}}), \\ \dfrac{2H_2}{\omega_R}\ddot{\delta}_2 + \dfrac{D_2}{\omega_R}\dot{\delta}_2 = A_2^{\mathrm{EN}} - K_{12}^{\mathrm{EN}}\sin(\delta_1-\delta_2-\gamma_{12}^{\mathrm{EN}}) - K_{23}^{\mathrm{EN}}\sin(\delta_2-\delta_3-\gamma_{23}^{\mathrm{EN}}), \\ \dfrac{2H_3}{\omega_R}\ddot{\delta}_3 + \dfrac{D_3}{\omega_R}\dot{\delta}_3 = A_3^{\mathrm{EN}} - K_{13}^{\mathrm{EN}}\sin(\delta_1-\delta_3-\gamma_{13}^{\mathrm{EN}}) - K_{23}^{\mathrm{EN}}\sin(\delta_2-\delta_3-\gamma_{23}^{\mathrm{EN}}). \end{cases} \quad (12)$$

2. Numerical results

Now rewrite the system of equations (12) as:

$$\begin{cases} \dot{x_1} = y_1, \\ \dot{y_1} = (A_1 - K_{12}\sin(x_1 - x_2 - \gamma_{12}) - K_{13}\sin(x_1 - x_3 - \gamma_{13}) - \dfrac{D_1}{\omega_R}y_1)\dfrac{\omega_R}{2H_1}, \\ \dot{x_2} = y_2, \\ \dot{y_2} = (A_2 - K_{12}\sin(x_1 - x_2 - \gamma_{12}) - K_{23}\sin(x_2 - x_3 - \gamma_{23}) - \dfrac{D_2}{\omega_R}y_2)\dfrac{\omega_R}{2H_2}, \\ \dot{x_3} = y_3, \\ \dot{y_3} = (A_3 - K_{13}\sin(x_1 - x_3 - \gamma_{13}) - K_{23}\sin(x_2 - x_3 - \gamma_{23}) - \dfrac{D_3}{\omega_R}y_3)\dfrac{\omega_R}{2H_3}. \end{cases} \quad (13)$$

Here x_n and $y_n$denote, respectively, the phases and the oscillator phase n ($n = 1, 2, 3$). Since the phases of the oscillators under consideration are constantly increasing in time, it is convenient to use periodic coordinates in the range from 0 to 2π to study the system.

Consider the first case of power system operation in which synchronous machines are in equilibrium, but the condition for synchronization of phase velocities $y_1 = y_2 = y_3$ is not satisfied. We use MATPOWER to define the physical network parameters, such as the total output capacity of the generator P_{gi}, Q_{gi} and the total power consumption load P_{li}, Q_{li}. The parameters of generators output capacity are, MW: $P_{g1} = 71.64$, $Q_{g1} = 27.05$, $P_{g2} = 163$, $Q_{g2} = 6.65$, $P_{g3} = 85$, $Q_{g3} = -10.86$. The parameters of the total power consumption load are, MW: $P_{l1} = 125$, $Q_{l1} = 50$, $P_{l2} = 90$, $Q_{l2} = 30$, $P_{l3} = 100$, $Q_{l3} = 35$. The effective network model parameters are $A_1 = -0.2276$, $A_2 = 1.1668$, $A_3 = 0.5635$, $K_{12} = 1.7089$, $K_{13} = 1.3361$, $K_{23} = 1.184$, $\gamma_{12} = -0.1875$, $\gamma_{13} = -0.1694$, $\gamma_{23} = -0.1964$, $H_1 = 23.64$, $H_2 = 6.4$, $H_3 = 3.01$, $D_{1,2,3} = 50$, $\omega_R = 314.1593$.

As an analysis tool, we apply the stroboscopic section method: the angular phase of $X_{2,3}$ oscillators is observed relative to the phase of the selected oscillator x_1. For this purpose, we choose a small range of values of the variable x_1 on the periodic plane ($0 \leqslant x_1 \leqslant 2\pi$) near $x_1 = x_1^*$. If the trajectory in a projection onto x_1 falls within this range $(x_1^* - \varepsilon; x_1^* + \varepsilon)$ ($\varepsilon \approx 1 \cdot 10^{-6}$), then the corresponding values of $X_{2,3}$ are plotted on the plot of the time dependence $X(t)$. In other words, when the phase of the oscillator is within the selected range of values $(x_1^* - \varepsilon; x_1^* + \varepsilon)$, the phase values of

the remaining oscillators are fixed. The obtained phase values are plotted against time $X_{2,3}(t)$. Analyzing the obtained data, we can draw a conclusion on the phase velocity change of the oscillators under study with respect to the given one.

Let us set the value of $x_1^* = 3$ and observe the phase change of the second and third oscillators relative to the first one, plotting the dependencies of their stroboscopic sections on time. In the case of phase synchronization the oscillators $X_{2,3}$ remain unchanged in the stroboscopic section. Furthermore, there are two typical cases of oscillator synchronization: when the phase-change velocities of all oscillators are equal or when they are in the multiple ratio. On the stroboscopic section the synchronization mode is represented by the straight line, that is parallel to the abscissa axis. The coincidence of the phase-change velocities should be checked separately. If there is no synchronization, the phases in the stroboscopic section will change. Thus, using the stroboscopic section, we can investigate the stability of the synchronization regime.

We now consider the behavior of the system as the initial conditions change. (Fig. 4, *a*) indicates that over time the system (13) is set to the stable operation mode of the power grid under the initial conditions $x_1 = 0$, $y_1 = 0$, $x_2 = 2.0944$, $y_2 = 0$, $x_3 = 4.1889$, $y_3 = 0$. We may specify initial conditions (for example, $x_1 = 0.1745$, $y_1 = 0$, $x_2 = 2.0944$, $y_2 = 0$, $x_3 = 4.1889$, $y_3 = 0$ на рис. 4, *b*) so that the system does not go into the stable operation mode over time. To illustrate the establishment of stable operation of the power grid (Fig. 4, *c*) versus its unstable operation (Fig. 4, *d*), we also indicate temporal realizations of the change in phase velocities of the selected oscillator. The figures show that phase velocities are constant in the stable operation mode and change periodically in the unstable one.

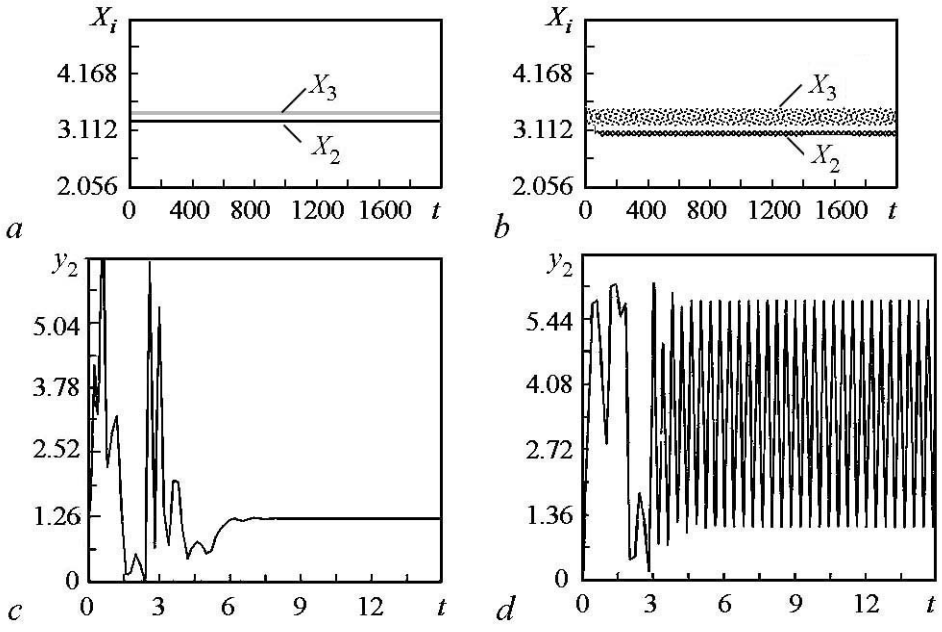

Fig. 4. Stroboscopic section of $X(t)$ for $x_1^* = 3$ for initial conditions $x_1 = 0$, $y_1 = 0$, $x_2 = 2.0944$, $y_2 = 0$, $x_3 = 4.1889$, $y_3 = 0$ (*a*), when initial conditions change for $x_1 = 0.1745$ (*b*). The time series of the change in the phase velocity of the second oscillator for initial conditions $x_1 = 0$, $y_1 = 0$, $x_2 = 2.0944$, $y_2 = 0$, $x_3 = 4.1889$, $y_3 = 0$ (*c*), and when the initial conditions change for $x_1 = 0.1745$ (*d*)

Now let's compare the modes of power grid operation for the various parameters of the oscillators. For this purpose, we change the output power values. We increase the output active power of the second generator P_{g2} from 163 to 219 MW. Thus, the new parameters of the effective network model are the following: $A_1 = -0.2276$, $A_2 = 1.7238$, $A_3 = 0.5635$, $K_{12} = 1.7274$, $K_{13} = 1.333$, $K_{23} = 1.1982$, $\gamma_{12} = -0.1912$, $\gamma_{13} = -0.1726$, $\gamma_{23} = -0.1959$, $H_1 = 23.64$, $H_2 = 6.4$, $H_3 = 3.01$, $D_{1,2,3} = 50$, $\omega_R = 314.1593$. We investigate the effective network model, using the abovementioned initial conditions that enable the stable mode operation. The analysis showed that when the active power is changed, the system remains in the stable operation mode of phase oscillators. Moreover, the synchronization mode is not disrupted even with the change of the initial conditions (Fig. 5, *a*). The temporal realization (Figure 5, *b*) shows that the phase velocities of the oscillators soon become constant and equal to each other $y_1 = y_2 = y_3 = 1.1769$. Thus, there is a synchronization in the system of coupled oscillators. To compare the eigenfrequencies of the oscillators, consider their deviation with respect to the reference frequency of 50 Hz. We calculate the eigenfrequencies for both modes of the power system operation, using the formula: $f_i = (1 + A_i/D_i)\omega_R/(2\pi)$. In the first case of synchronization with different phase velocities, the eigenfrequencies were the following: $f_1 = 49.77$, $f_2 = 51.17$, $f_3 = 50.56$ Hz. In the synchronous mode with identical phase velocities the eigenfrequencies were the following: $f_1 = 49.77$, $f_2 = 51.72$, $f_3 = 50.56$ Hz. It should be noted that in both cases the eigenfrequencies of the corresponding oscillators f_1 и f_3 were chosen to be close to the value of the reference frequency, whereas the eigenfrequency of the second oscillator f_2 differs significantly from it. The increase in the generator output power led to an increase in its own rotational speed. Generally speaking, such an increase in frequency would result in additional heat generation in the synchronous machine. When designing such a network, it should be taken into consideration, as it may cause the generator to overheat.

Let's perform several different tests for a more detailed consideration of the differences between the two synchronous modes of power grid operation [11]. First consider

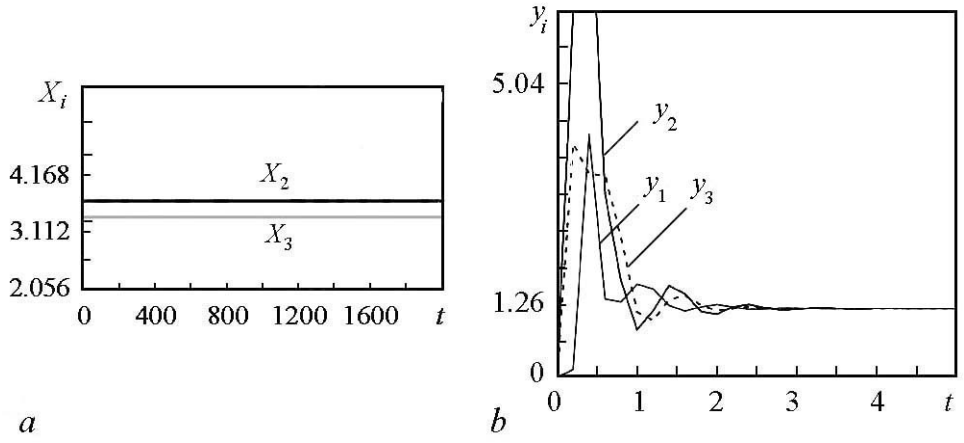

Fig. 5. Stroboscopic section $X(t)$ for $x_1^* = 3$ for any initial conditions (*a*), time series of the phase velocity change for any initial conditions (*b*)

the system under the influence of additive white Gaussian noise. We add the noise to each equation of the system (13) and thus obtain the following equations:

$$\begin{cases} \dot{x_1} = y_1, \\ \dot{y_1} = (A_1 - K_{12}\sin(x_1 - x_2 - \gamma_{12}) - K_{13}\sin(x_1 - x_3 - \gamma_{13}) - \dfrac{D_1}{\omega_R} y_1 + \sqrt{2\sigma_1}\xi_1(t))\dfrac{\omega_R}{2H_1}, \\ \dot{x_2} = y_2, \\ \dot{y_2} = (A_2 - K_{12}\sin(x_1 - x_2 - \gamma_{12}) - K_{23}\sin(x_2 - x_3 - \gamma_{23}) - \dfrac{D_2}{\omega_R} y_2 + \sqrt{2\sigma_2}\xi_2(t))\dfrac{\omega_R}{2H_2}, \\ \dot{x_3} = y_3, \\ \dot{y_3} = (A_3 - K_{13}\sin(x_1 - x_3 - \gamma_{13}) - K_{23}\sin(x_2 - x_3 - \gamma_{23}) - \dfrac{D_3}{\omega_R} y_3 + \sqrt{2\sigma_3}\xi_3(t))\dfrac{\omega_R}{2H_3}, \end{cases} \tag{14}$$

where σ_i is the noise intensity, ξ_i is an independent noise source.

To study the effect of noise on the system, we choose the time interval from t_1=500 to $t_2 = 1500$ ($\sigma_{1,2,3} = \sigma_0$ at $T \in [t_1, t_2]$, and $\sigma_{1,2,3} = 0$ at $t \notin [t_1, t_2]$) and examine the modes at high noise intensity $\sigma_{1,2,3} \sim 0.1$. Fig. 6, *a* shows that, in a stable operation mode with different phase velocities there might be the loss of oscillator stability after Gaussian noise exposure has stopped. This phenomenon can also be observed at sufficiently low noise intensities. Furthermore, the probability of the disruption of stable operation

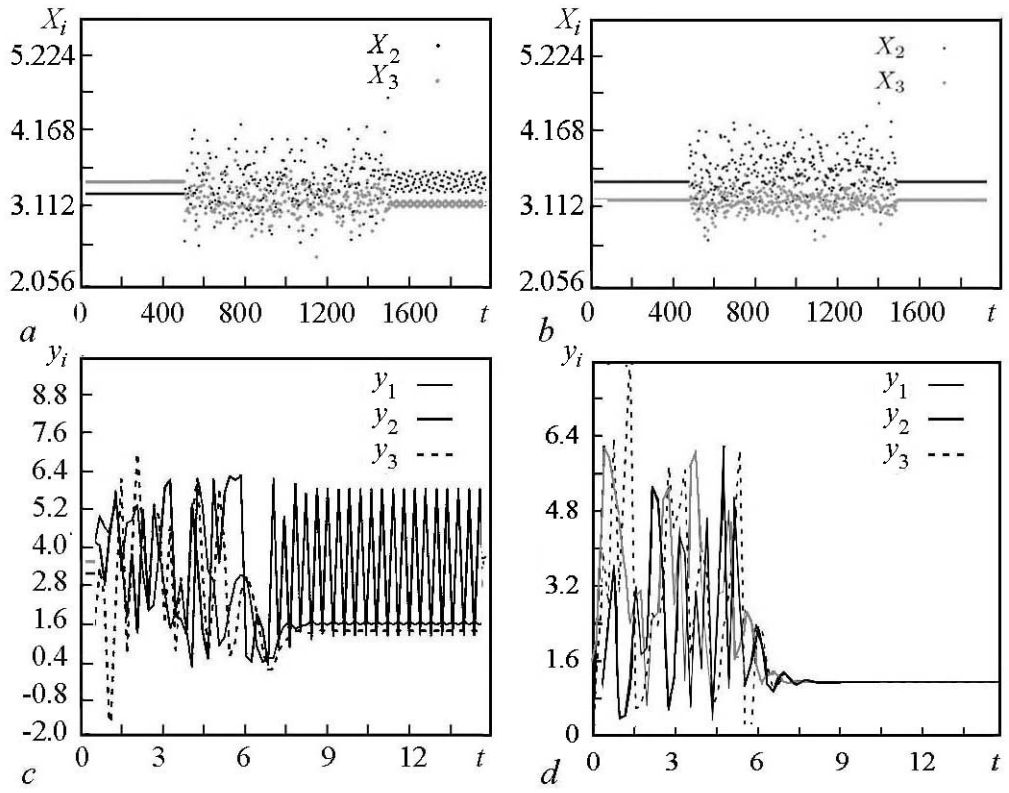

Fig. 6. (*a, b*) – Stroboscopic sections $X(t)$ for $x_1^* = 3$ for synchronous modes with different and identical phase velocities, respectively, black dots – stroboscopic section for X_2, gray – for X_3, (*c, d*) are the time series of the phase velocities of stable regimes with different and identical phase velocities, respectively

increases with the noise increase in the system. The synchronous mode showed very high noise immunity (Fig. 6, *b*). It should be noted, however, that this mode is resistant to noise effects even in the initial period of time (Fig. 6, *d*), when the phase velocity undergoes significant changes, but tends to equilibrium. The noise effect on a synchronous mode with different phase velocities at the initial instant of time results in the loss of oscillator stability (Fig. 6, *c*).

It is worth considering the behavior of the system under the influence of a rectangular pulse, which simulates power surges in the power grid. We add a pulse to the second equation of the system under consideration for both synchronous modes (with different behavior of phase velocities). The equations of the system (13) will take the form:

$$\begin{cases} \dot{x_1} = y_1, \\ \dot{y_1} = (A_1 - K_{12}\sin(x_1 - x_2 - \gamma_{12}) - K_{13}\sin(x_1 - x_3 - \gamma_{13}) - \dfrac{D_1}{\omega_R} y_1)\dfrac{\omega_R}{2H_1}, \\ \dot{x_2} = y_2, \\ \dot{y_2} = (A_2 - K_{12}\sin(x_1 - x_2 - \gamma_{12}) - K_{23}\sin(x_2 - x_3 - \gamma_{23}) - \dfrac{D_2}{\omega_R} y_2 + f_1(\tau))\dfrac{\omega_R}{2H_2}, \\ \dot{x_3} = y_3, \\ \dot{y_3} = (A_3 - K_{13}\sin(x_1 - x_3 - \gamma_{13}) - K_{23}\sin(x_2 - x_3 - \gamma_{23}) - \dfrac{D_3}{\omega_R} y_3)\dfrac{\omega_R}{2H_3}, \end{cases} \quad (15)$$

where $f_1(\tau)$ is a rectangular pulse of a given amplitude and duration. Let us determine the pulse duration τ=1000, the pulse-on time t=500 and the pulse action amplitude A=1.9.

The application of the rectangular pulse to the system with unequal phase velocities causes the disruption of its stable operation, so the phase velocities of all the oscillators are changing according to the periodic law. After the application of the pulse has ceased, the system does not return to its original state and continues to operate in asynchronous mode (Fig. 7, *a*). Perturbation of the system in synchronous mode leads to the different behavior of the oscillators. At the initial stage of the perturbation time, there is a short

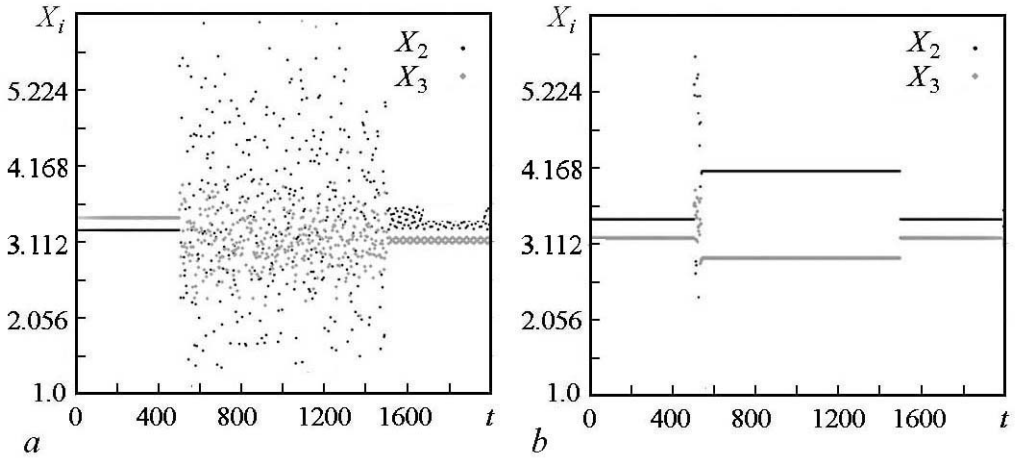

Fig. 7. Stroboscopic sections $X(t)$ for $x_1^* = 3$ for stable regimes in the case of different (*a*) and identical (*b*) phase velocities. Black points of the stroboscopic section mark X_2, gray points – X_3

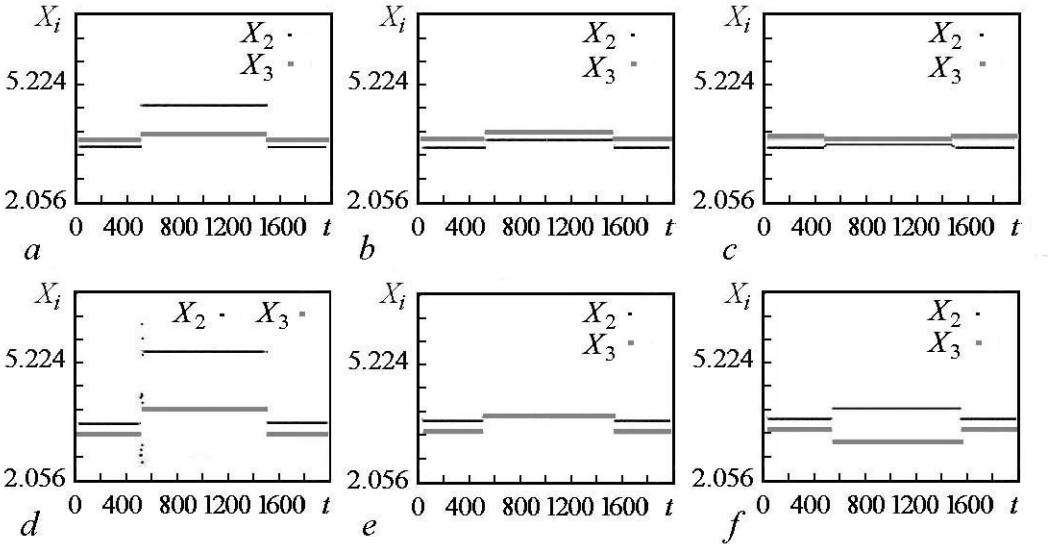

Fig. 8. Stroboscopic sections $X(t)$ for $x_1^* = 3$ for synchronous operation with different (*a, b, c*) and identical (*d, e, f*) phase velocities when removed the next links: K_{12} (*a, d*); K_{13} (*b, e*); K_{23} (*c, f*). Black dots denote the stroboscopic section for X_2, and gray ones for X_3

perturbation of phase velocities and the system reaches an equilibrium. That is, a new synchronous mode is formed (Fig. 7, *b*). After the application of the pulse has ceased, the power grid returns to its original stable operation mode.

In real power grids decoupling between the generators should also be taken into account. To simulate this situation, we eliminate one coupling in the system of equations (13). Let's eliminate one coupling in the time interval from $t_1 = 500$ to $t_2 = 1500$, thus simulating the emergency mode caused by transmission line breaks. The inclusion of the coupling term corresponds to the restoration of the transmission line.

As can be seen from Fig. 8, both stable modes behave in the same way: when one coupling is eliminated, the oscillators switch to the new stable operation mode and return to their previous stable state once the coupling has been restored. It was also found that phase velocities are synchronized in the absence of K_{12} or K_{13} couplings (Fig. 8, *a*, *c*). That is, the initial mode is replaced by the mode with identical phase velocities during the decoupling.

Concluding Remarks

An effective network model was considered, focusing on the behavior of coupled generators, while eliminating from consideration the network load. The aim of the study is to analyze the stable operation modes of the power grid under the influence of various external factors. Firstly, the model under consideration can demonstrate different modes of operation in relation to the initial conditions. It is shown that by adjusting the generator output power it is possible to insure the stability of the system, which is resistant to variations of the initial conditions. Moreover, it was found that the functioning of such a system is less sensitive to various external factors. Secondly, the influence of various external factors on two key operation modes (synchronous and asynchronous) was considered. The system was examined under the influence of additive white Gaussian noise

and rectangular pulse in a given time interval. Furthermore, the steady-state modes have been investigated corresponding to the topology changes. Thus, the power grid in the synchronous mode is independent of initial conditions and is more resistant to negative factors in comparison with the mode of synchronization with different phase velocities. In this regard, it is worth drawing attention to the deviation of eigenfrequencies of the generators with respect to the reference frequency. The frequency difference of more than ± 2 Hz results in the increased accumulation of heat in the synchronous machine and, consequently, in an early failure of the generator. In the investigated stable operation modes the frequency difference is within 4% of the 50 Hz reference frequency. Thus, the study of the power grid of three coupled generators has demonstrated the behavior of the key modes of operation of power grids and has shown the possibility for optimizing the energy network by adjusting the generator output power parameter.

Annex

Consider the swing equation, suggested in [7]. To derive the equation of motion and describe the dynamics of the generator, we may write the following equation for the rotational velocity of the rotor (the rotational velocity is equal to the rotor torque):

$$J\ddot{\delta} = \bar{T}_{\mathrm{m}} - D_{\mathrm{m}}\omega - \frac{1}{R}\Delta\omega - D_{\mathrm{e}}\Delta\omega - T_{\mathrm{e}}, \tag{An.1}$$

where J is the moment of inertia in [kg·m^2]; δ is the rotor angle relative to a frame rotating at the reference frequency ω_R, [rad/s]; $\bar{T}_{\mathrm{m}}$ is the mechanical torque, [N·m]; D_{m} is the damping coefficient in [N·m·s]; ω is rotor angular frequency, [rad/s]; R is the regulation parameter in [rad/ (N·m·s)], characterizing the proportional frequency control by a governor with the frequency deviation $\Delta\omega = \omega - \omega_R$; D_{e} is the damping coefficient in [N·m·s], for the electrical effect of the generator's damper windings, and T_{e} is the typically decelerating torque in [N·m] due to electrical load in the network. Noting that $\omega - \omega_R = \Delta\omega$, we can rewrite the equation as (An.1) as

$$J\ddot{\delta} + \bar{D}\delta = \bar{T}_{\mathrm{m}} - T_{\mathrm{e}}, \tag{An.2}$$

where $\bar{D} = D_{\mathrm{m}} + D_{\mathrm{e}} + 1/R$ is frictional loss at the reference frequency and $\bar{T}_{\mathrm{m}} = T_{\mathrm{m}} - D_{\mathrm{m}}\omega_R$ is the net mechanical torque. Multiplying both sides by ω and using the fact that torque in [N·m] multiplied by angular velocity in radians per second gives power in watts, the equation (An.2) can be written in terms of power:

$$J\omega_R\ddot{\delta} + \bar{D}\omega_R\dot{\delta} = \frac{\omega_R}{\omega}(T_{\mathrm{m}}\omega - T_{\mathrm{e}}\omega) \approx \bar{P}_{\mathrm{m}} - \bar{P}_{\mathrm{e}}. \tag{An.3}$$

Next we define the right-hand side of the equation in terms of power $\bar{P}_{\mathrm{m}} = T_{\mathrm{m}}\omega$ and $\bar{P}_{\mathrm{e}} = T_{\mathrm{e}}\omega$. Then we assumed the factor ω_R/ω to be nearly equal to one, i.e., that the generator's frequency ω is close to the reference frequency ω_R. We now divide both sides of the equation (An.3) by the rated power P_R (used as a reference) as normalization procedure to make P_{m} and P_{e} per unit quantities. The factor $J\omega_R$ then becomes $2H/\omega_R$, where we defined the inertia constant $H = W/P_R$ (in seconds) and the kinetic energy of the rotor $W = J\omega_R^2/2$ (in joules). We define the combined damping coefficient

as $D = \omega_R / P_R$ (in seconds).We then obtain the desired equation known as the swing equation

$$\frac{2H}{\omega_R}\ddot{\delta} + \frac{D}{\omega_R}\dot{\delta} = P_{\mathrm{m}} - P_{\mathrm{e}}, \qquad \text{(An.4)}$$

which is the fundamental equation of motion for a generator. The term P_{m} represents the net mechanical power input to the rotor, while P_{e} represents the electrical power demanded by the rest of the network and includes terms that depend explicitly on δ, and the state variables of the other generators and loads in the network. There has been substantial effort in the power systems literature [12] to model the dynamical behavior of the generator.s internal magnetic flux, which affects the value P_{e}. One may also need to include the nonlinear dynamics of the governor that controls the generator frequency and the excitation system that controls the voltage magnitude at the generator terminal. Thus, P_{e} is a dynamic quantity, which may need to be accounted for in high-accuracy simulations of power systems.

References

1. Stadler I. Power grid balancing of energy systems with high renewable energy penetration by demand response. *Utilities Policy*, 2008, vol. 16, no. 2, pp. 90–98.
2. Anvari M., Lohmann G., Wächter M. Short term fluctuations of wind and solar power systems. *New Journal of Physics*, 2016, vol. 18, no. 6, p. 063027.
3. Menck P.J., Heitzig J. How dead ends undermine power grid stability. *Nature communications*, 2014, vol. 5, p. 3969.
4. Pedersen R., Findrik M., Sloth C. Network condition based adaptive control and its application to power balancing in electrical grids. *Sustainable Energy, Grids and Networks,* 2017, vol. 10, pp. 118–127.
5. Rohden M., Witthaut D., Timme M. Curing critical links in oscillator networks as power grid models. *New Journal of Physics*, 2017, vol. 19, no. 1, p. 013002.
6. Usoltsev A.A. General Electrical Engineering: Textbook. St. Petersburg: St. Petersburg State University. ITMO. 2009. 301 s. (in Russian).
7. Nishikawa T., Motter A.E. Comparative analysis of existing models for power-grid synchronization. *New Journal of Physics*, 2015, vol. 17, no. 1, p. 015012.
8. Dorfler F., Bullo F. Kron reduction of graphs with applications to electrical networks. *IEEE Transactions on Circuits and Systems I: Regular Papers*, 2013, vol. 60, no. 1, pp. 150–163.
9. Zimmerman R.D., Murillo-Sánchez C.E., Thomas R.J. MATPOWER: Steady-state operations, planning, and analysis tools for power systems research and education. *IEEE Transactions on power systems*, 2011, vol. 26, no. 1, pp. 12–19.
10. Meleshkin G.A., Merkuriev G.V. Stability of Power Systems. Theory: Monograph. SPb.: NOU «Center for the Training of Energy Personnel», 2006, 350 s. (in Russian).
11. Rohden M., Sorge A., Witthaut D. Impact of network topology on synchrony of oscillatory power grids. *Chaos: An Interdisciplinary Journal of Nonlinear Science*, 2014, vol.24, no.1, p.013123.
12. Khrushchev Yu.V., Zapodovnikov K.I., Yushkov A.Yu. Electromechanical Transitive Processes in Electro-Energy Systems: Training manual. Tomsk: Publishing house of Tomsk Polytechnic University. 2010 (in Russian).